Biochemistry and Biophysics Reports 39 (2024) 101799

Contents lists available at ScienceDirect

Biochemistry and Biophysics Reports

journal homepage: www.elsevier.com/locate/bbrep

Membrane-anchored intracellular insulin receptor or insulin-like growth factor-1 receptor elicits ligand-independent downstream signaling

Akiko Sotozono [a,b], Kazuhiko Namekata [a,*], Xiaoli Guo [a], Youichi Shinozaki [a], Chikako Harada [a], Takahiko Noro [a,b], Tadashi Nakano [b], Takayuki Harada [a]

[a] Visual Research Project, Tokyo Metropolitan Institute of Medical Science, Tokyo, Japan
[b] Department of Ophthalmology, The Jikei University School of Medicine, Tokyo, Japan

ARTICLE INFO

Keywords:
AKT
ERK
Farnesylation
Insulin receptor
Insulin-like growth factor-1 receptor

ABSTRACT

Neurodegenerative diseases including glaucoma affect insulin signaling, and insulin treatment has been shown to reverse the neurodegenerative loss of dendritic complexity in retinal ganglion cells. Therefore, strategies for enhancing or maintaining insulin signaling are worth pursuing to establish new therapies for these diseases. In the present study, we generated constitutively active insulin receptor (F-iIR) and insulin-like growth factor-1 receptor (F-iIGF1R) using a system that forces membrane localization of the intracellular domains of these receptors by farnesylation. Immunohistochemistry and Western blot analysis revealed that F-iIR and F-iIGF1R caused the activation of ERK and AKT in the absence of ligands *in vitro*. Our results suggest that *in vivo* effects of F-iIR and F-iIGF1R on the progression of neurodegenerative diseases should be investigated in the future.

1. Introduction

Aberrant or insufficient insulin signaling has been associated with glaucoma, the leading cause of blindness [1]. Insulin crosses the blood–brain barrier and can influence a number of physiological brain processes including neuronal survival, neurotransmission, and cognitive performance [2]. Hence, insulin signaling may be potentially targeted for disease modification [3]. Indeed, insulin or insulin-like growth factor-1 (IGF1) have been reported to be neuroprotective in glaucoma and other rodent CNS injury models [4]. Using an *in vivo* model of traumatic nerve injury, Agostinone et al. [4] demonstrated that daily insulin treatment starting 3 days post-injury reverses the loss of dendritic complexity and somatic atrophy of retinal ganglion cells (RGCs) with insulin acting through the PTEN/PI3K/Akt/mTOR pathway. These studies indicate that strategies enhancing or maintaining insulin signaling are worth pursuing to establish new therapies for neurodegenerative diseases including glaucoma.

We recently developed a system that forces membrane localization of the intracellular domain of tropomyosin receptor kinase B (iTrkB) by farnesylation (F-iTrkB). Overexpression of F-iTrkB results in constitutive activation of downstream signaling pathways in the absence of TrkB's ligand, brain-derived neurotrophic factor (BDNF) [5]. This system overcomes the small size limitation of the genome packaging in adeno-associated virus (AAV) because it does not express full-length receptor, and it allows high expression of the transgene. Using AAV-mediated gene therapy in the eyes, we demonstrated that F-iTrkB expression enhances neuroprotection in mouse models of glaucoma, stimulates robust axon regeneration after optic nerve injury, and is effective in an optic tract transection model. Our study implies that this system might be also applicable for other gene therapies [5].

In the present study, we generated constitutively active insulin receptor (F-iIR) and insulin-like growth factor-1 receptor (F-iIGF1R) using the same system that we used to generate F-iTrkB. The current consensus from optic nerve injury studies, other glaucoma models, and clinical data is that dendritic retraction is an early event in the pathology of glaucoma, starting before somatic loss, axon pathology, and overt functional changes [6–10]. Using an optic nerve injury model, Agostinone et al. [4] reported that insulin treatment successfully reverses the loss of dendritic complexity and provided the first evidence of successful dendritic regeneration in retinal neurons. In their study, insulin was administered by daily intraperitoneal injections or eye drops for four days. Given that F-iTrkB was effective in stimulating robust axon regeneration as a monogenic treatment [5,11], there is a high possibility that gene therapy overexpression of F-iIR or F-iIGF1R might be consecutively effective for promoting dendritic regeneration. As a first step to test our hypothesis *in vivo*, we investigated whether downstream

* Corresponding author. Visual Research Project, Tokyo Metropolitan Institute of Medical Science, 2-1-6 Kamikitazawa, Setagaya-ku, Tokyo, 156-8506, Japan.
E-mail address: namekata-kz@igakuken.or.jp (K. Namekata).

https://doi.org/10.1016/j.bbrep.2024.101799
Received 23 April 2024; Received in revised form 17 July 2024; Accepted 22 July 2024

signaling pathways of IR and IGR1R are activated by these constructs using immunohistochemistry and western blotting analysis.

2. Materials and methods

2.1. Plasmids

gBlock DNA fragments (IDT, Burlington, MA, USA) of the intracellular domain of IR (iIR) or IGF1R (iIGF1R) were synthesized. The DNA sequences were obtained from GenBank (NM_010568.3 and NM_000875.2). A myc-tag was attached to the N-terminus of these fragments for detection by immunostaining and immunoblot analysis. A K-Ras-derived farnesylation signal was add to the C-terminus for membrane localization. Each construct was expressed under the CAG promoter.

2.2. Transfection and immunocytochemistry analysis

Cos-7 cells (African green monkey kidney fibroblast-like cell) and Neuro2A cells (Mouse neuroblastoma cell) were cultured on cover glass in culture medium (DMEM with high glucose, 10 % FBS, 100 unit/ml penicillin, 100 μg/ml streptomycin). Transient transfection in both cell lines was performed using Polyethylenimine HCl Max (Polyscience, Warrington, PA, USA). The transfection efficiencies in Cos-7 and Neuro2A cells were 65.2 ± 4.7 % and 46.8 ± 6.3 %, respectively. After transfection for 20–24 h, cells were serum-starved for 6 h, fixed for 20 min in 4 % formalin and stained with the following primary antibodies: anti-c-Myc (M192, MBL,Tokyo, Japan), anti-ERK (4695, Cell Signalling Technology, Danvers, MA, USA), anti-AKT (9272, Cell Signalling Technology), anti-Phospho ERK (4370, Cell Signalling Technology) and anti-Phospho AKT (9271, Cell Signalling Technology). Alexa Fluor–conjugated donkey anti-rabbit IgG and anti-mouse IgG (1:1000; Thermo Fisher Scinetific, Waltham, MA, USA) were used as secondary antibodies. After immunostaining, images were obtained with a BZ-9000 fluorescence microscope (Keyence, Osaka, Japan).

2.3. Transfection and immunoblot analysis

Cos-7 cells were cultured in 48-well culture plate with culture medium (DMEM with high glucose, 10% FBS, 100 unit/ml penicillin, 100 mg/ml streptomycin). Transient transfection in both cell lines was performed using Polyethylenimine HCl Max (Polyscience). For signal transduction analyses, cells were serum-starved for 6 h before cell lysis. Cells were lysed in SDS-PAGE loading buffer (2 % SDS, 62 mM Tris pH6.8, 15 % glycerol, 5 % 2-mercaptethanol) and were heated at 100 °C for 5 min. Proteins were separated by SDS-PAGE using 5–20 % gradient gel and transferred to an Immobilon-P filter (IPVH00010, EMD Millipore, Burlington, MA, USA). Membranes were incubated with antibodies against pERK, pAKT, ERK, AKT, pIR/pIGF1R (3021, Cell Signaling Technology), pIRS-1 (3070, Cell Signaling Technology), IRS-1 (3407, Cell Signaling Technology), myc, actin (612656, BD Biosciences, Franklin Lakes, NJ, USA) in PBS containing 0.05 % Tween 20 (PBS-T) and 2.5 % skimmed milk. Membranes were washed in PBS-T and incubated with horseradish peroxidase–conjugated secondary antibodies against mouse IgG (1:1000; Cell Signaling Technology), rabbit IgG (1:1000; Cell Signaling Technology). Quantitative analysis was carried out using ImageJ version 2.0.0 [12].

2.4. Pull-down assay

Cos-7 cells in 6-well culture plate transfected with plasmids of interest were lysed with a lysis buffer (25 mM Tris [pH 7.4], 150 mM NaCl, 1 % Triton X-100) and centrifuged at 16,000 g for 10 min. The supernatant was incubated with glutathione Sepharose 4B resin (17513201, Cytiba, Marlborough, MA, USA) for 30 min at 4 °C with gentle agitation. After 4 times of washing, the precipitated samples were subjected to immunoblot analysis using anti-myc antibody.

2.5. Statistical analysis

Statistical analyses were performed using Prism 9 software (GraphPad Software, Boston, MA, USA). Data are represented as means ± SEMs. For statistical analysis, 6 samples were prepared in each group. Significance was determined using the non-parametric Kruskal-Wallis and post hoc Dunn's Multiple comparison tests. A value of $P < 0.05$ was considered statistically significant.

3. Results

3.1. Membrane-anchored intracellular IR and IGF1R activate endogenous ERK and AKT in the absence of insulin

The insulin receptor (IR) is localized at the plasma membrane and possesses a single transmembrane domain. Binding of insulin to its extracellular domain activates the kinase domain in the intracellular region of the receptor, leading to the activation of Ras-ERK and PI3K-AKT signaling pathways. Since the intracellular domain of IR (iIR) plays an important role in signal transduction, we made a construct consisting of the iIR (Fig. 1A). To localize the iIR to the plasma membrane, we attached a farnesylation signal sequence, CAAX, to the iIR (F-iIR in Fig. 1A). A membrane localized version of the intracellular domain of the IGF1 receptor (IGF1R) was also generated using a similar strategy (F-iIGF1R in Fig. 1A). We then transfected these constructs into Cos-7 cells and assessed their overexpression using an anti-myc antibody. After transfection, myc-tagged F-iIR, F-iIGF1R, iIR, and iIGF1R were detected in Cos-7 cells (upper panel in Fig. 1B). However, it was difficult to distinguish whether the farnesylated forms localized at the plasma membrane due to the flat morphology of Cos-7 cells. Hence, we also evaluated the subcellular localization of these proteins using Neuro2A cells, which have a more spherical morphology. Farnesylated forms (F-iIR and F-iIGF1R) were clearly detected at the cell periphery of Neuro2A cells, whereas non-farnesylated iIR and iIGF1R were expressed diffusely in the cytoplasm (lower panel in Fig. 1B).

To investigate whether the farnesylated intracellular domains can activate ERK and AKT, Cos-7 cells were transfected with F-iIR, iIR, F-iIGF1R, or iIGF1R plasmids. After fixation, phosphorylated ERK in the cells was detected using anti-phosphorylated ERK antibody. Immunostaining analysis revealed that phosphorylated ERK was detected in Cos-7 cells co-transfected with F-iIR and ERK plasmids, whereas Cos-7 cells transfected with non-farnesylated iIR plasmid failed to induce ERK phosphorylation (upper panel in Fig. 2A). Similar effects were observed in Cos-7 cells transfected with F-iIGF1R and iIGF1R (lower panel in Fig. 2A). AKT phosphorylation was also evident in cells transfected with F-iIR or F-iIGF1R plasmids, but not with iIR or iIGF1R (Fig. 2B). The percentage of cells positive for phosphorylated ERK was 59.1 ± 4.1 % and 57.6 ± 7.6 % in cells transfected with F-iIR or F-iIGF1R respectively, and the percentage of phosphorylated AKT positive cells was 64.2 ± 1.4 % and 58.4 ± 4.2 %, respectively. These results suggest that overexpression of the membrane-bound intracellular domains of IR or IGF1R can induce ERK and AKT activation in the absence of insulin.

3.2. Membrane-anchored intracellular IR and IGF1R activate endogenous downstream signal transduction in the absence of insulin

Upon binding to its ligand, the full-length IR dimer is activated, transphosphorylated and then forms a complex with IRS-1, resulting in phosphorylation of IRS-1, which is required for the induction of downstream signaling. We next investigated in more detail the effects of F-iIR and F-iIGF1R on endogenous downstream signal transduction through immunoblot analysis. Cos-7 cells were transfected with either F-iIR or iIR, and phosphorylated form of F-iIR and IRS-1 were assessed by immunoblot analysis. We found that F-iIR was phosphorylated and there

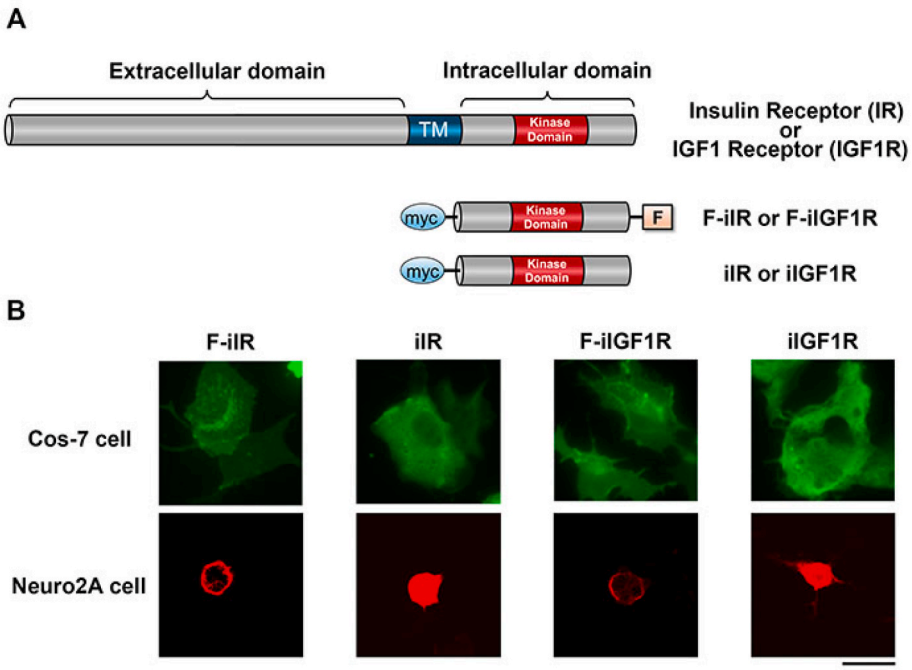

Fig. 1. Farnesylated intracellular domains of IR and IGF1R. **A:** Schematic diagram of IR and IGF1R constructs used in this study. TM, transmembrane domain; myc, myc-tag; F, farnesylation signal; F-iIR, farnesylated intracellular domain of IR; F-iIGF1R, farnesylated intracellular domain of IGF1R.
B: Cellular localization of IR and IGF1R in Cos-7 and Neuro2A cells transfected with the indicated plasmids. Overexpressed proteins were detected with anti-myc atntibody. Membrane localized F-iIR and F-iGF1R were more clearly detected in Neuro2A cells than Cos-7 cells. Scale bar: 20 μm.

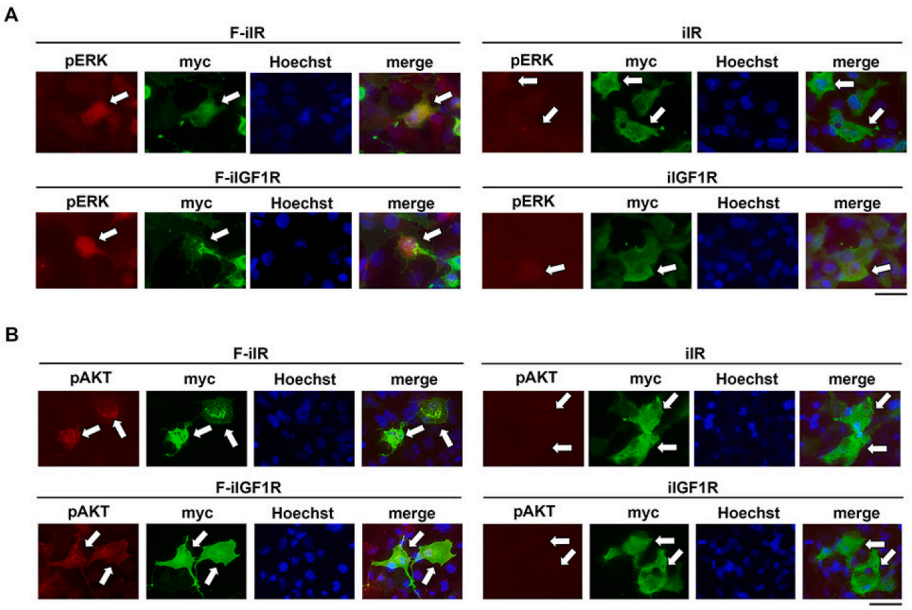

Fig. 2. Immunocytochemical analysis of ERK and AKT activation by F-iIR and F-iIGF1R in the absence of insulin. **A:** Activation of ERK by F-iIR or F-iIGF1R. Immunocytochemical analysis demonstrated ERK phosphorylation in Cos-7 cells expressing myc-tagged F-iIR or F-iIGF1R (arrows). ERK phosphorylation was absent in Cos-7 cells expressing myc-tagged iIR or iIGF1R (arrows).
B: Activation of AKT by F-iIR or F-iIGF1R. Immunocytochemical analysis demonstrated AKT phosphorylation in Cos-7 cells expressing myc-tagged F-iIR or F-iIGF1R (arrows). AKT phosphorylation was absent in Cos-7 cells expressing myc-tagged iIR or iIGF1R (arrows). Scale bar: 20 μm.

was increased phosphorylation of IRS-1 compared with controls, whereas iIR did not (left panels in Fig. 3A and Supplementary Fig. 1). In addition, phosphorylated ERK and AKT was also increased by F-iIR compared with controls, whereas iIR did not (left panels in Fig. 3B and Supplementary Fig. 2). Similarly, F-iIGF1R was phosphorylated and induced phosphorylation of IRS-1, ERK and AKT while iIGF1R did not (right panels in Fig. 3A and B and Supplementary Figs. 1–2). Quantitative analysis revealed that F-iIR significantly increased phosphorylation of endogenous ERK (3.01 ± 0.27 fold) and AKT (6.06 ± 0.78 fold) compared with controls (Fig. 4A). F-iIGF1R also significantly increased phosphorylation of endogenous ERK (3.06 ± 0.29 fold) and AKT (4.48 ± 0.28 fold) compared with controls (Fig. 4B). These results suggest that

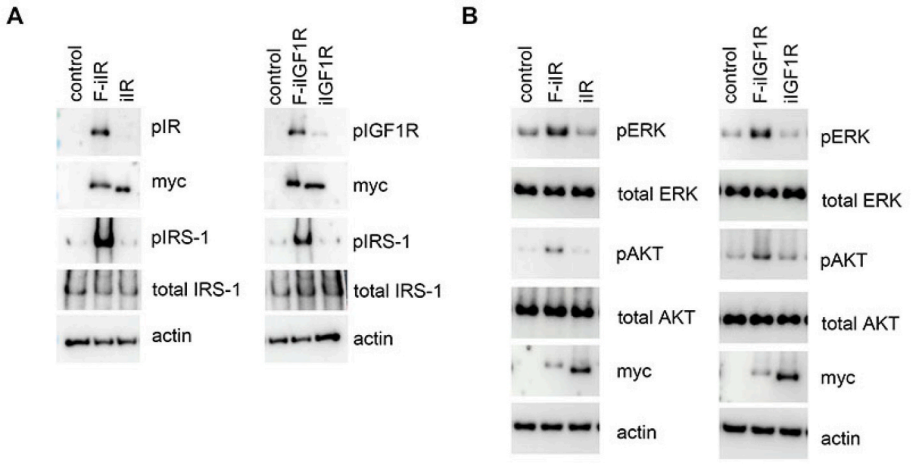

Fig. 3. The effect of kinase activity of F-iIR or F-iIGF1R on downstream signal transduction. **A:** Representative immunoblot images of pIR or pIGF1R, myc, pIRS-1, total IRS-1 and actin in Cos-7 cells transfected with plasmids expressing F-iIR, iIR, F-iIGF1R or iIGF1R.
B: Representative immunoblot images of pERK, total ERK, pAKT, total AKT, myc and actin in Cos-7 cells transfected with plasmids expressing F-iIR, iIR, F-iIGF1R or iIGF1R.

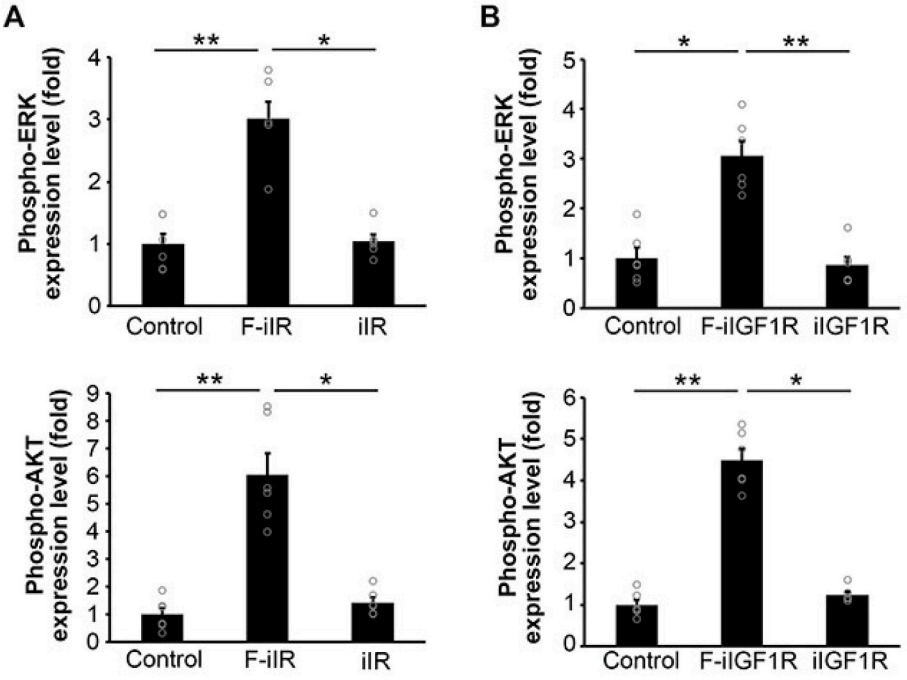

Fig. 4. Quantification of ERK and AKT activation by F-iIR and F-iIGF1R. **A:** Quantification of the relative amounts of phosphorylated ERK (upper) or phosphorylated AKT (lower) in Cos-7 cells transfected with F-iIR and iIR expressing plasmids.
B: Quantification of the relative amounts of phosphorylated ERK (upper) or phosphorylated AKT (lower) in Cos-7 cells transfected with F-iIGF1R and iIGF1R expressing plasmids.
The non-parametric Kruskal-Wallis and post hoc Dunn's Multiple comparison tests were used. n = 6 per experimental condition. $^{**}P < 0.01$; $^{*}P < 0.05$.

both F-iIR and F-iIGF1R are able to activate endogenous signal transduction pathways.

We also investigated whether F-iIR or F-iIGF1R forms a dimer using Cos-7 cells. A pull-down assay revealed that neither F-iIR nor F-iIGF1R bound to F-iIR-GST or F-IGF1R-GST (Fig. 5). These results suggest that F-iIR or F-iIGF1R does not form a stable dimer, and their trans-phosphorylation may be induced by transient interactions.

4. Discussion

In the present study, we generated two constructs of insulin receptor and IGF-1 receptor mutants (F-iIR and F-iIGF1R) to constitutively activate intracellular signaling in the absence of their ligands, insulin or IGF-1. These constructs were developed using the same system employed recently to make F-iTrkB [5]. F-iIR and F-iIGF1R were myc-tagged intracellular domain of receptors and attached fanesylation signal sequence at C-terminus. Immunohistochemical analysis revealed that both F-iIR and F-iIGF1R, but not iIR and iIGF1R, were localized at plasma membrane. In addition, western blotting analysis revealed that both F-iIR and F-iIGF1R, but not iIR and iIGF1R, activated ERK and AKT downstream signaling pathways. These findings suggest that membrane localization is a critical event for the activation of ERK/AKT signaling by

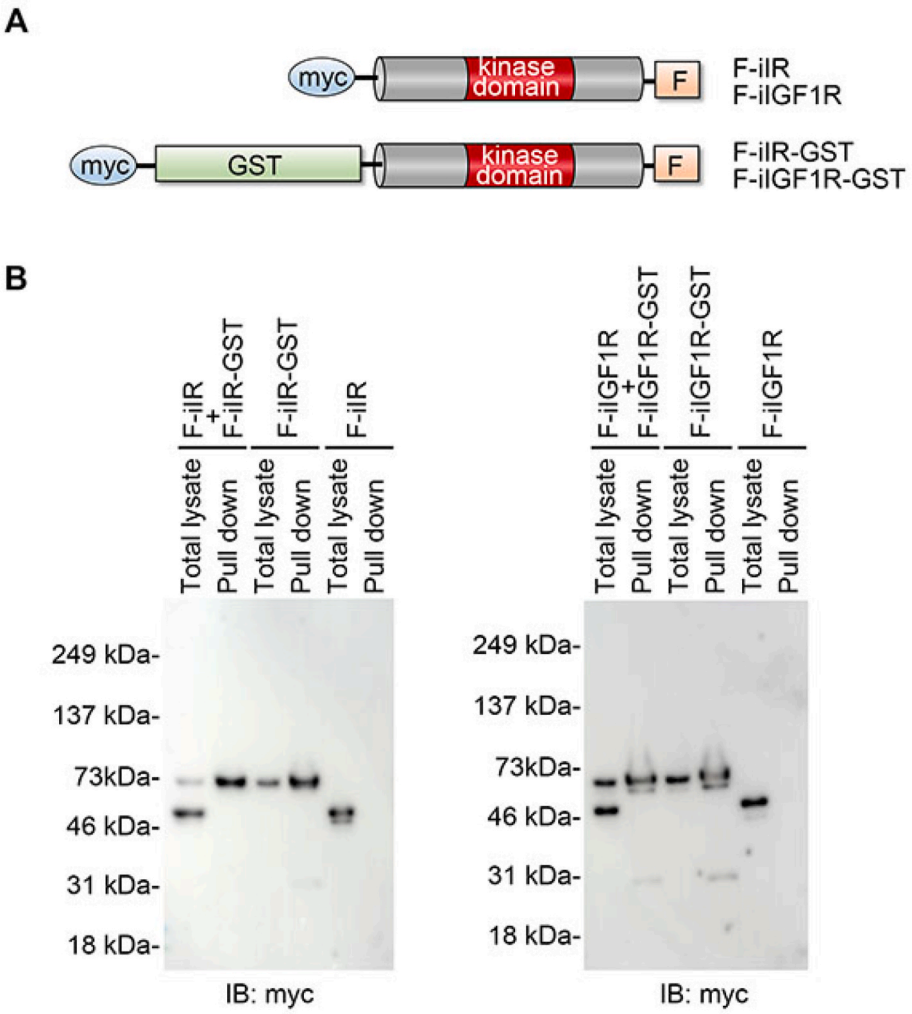

Fig. 5. Characterization of F-iIR and F-iIGF1R. **A:** Schematic diagram of GST-tagged F-iIR (F-iIR-GST) and F-iIGF1R (F-iIGF1R-GST) constructs used in this study. **B:** No detection of F-iIR or F-iIGF1R dimers. Cos-7 cells were cotransfected with F-iIR-GST and F-iIR (left panel) or F-iIGF1R-GST and F-iIGF1R (right panel), followed by a GST pull-down assay. The pull-down sample was subjected to immunoblot analysis.

F-iIR and F-iIGF1R. Indeed, we previously reported that the farnesylated intracellular domain of TrkA and TrkB also activate intracellular ERK and AKT signaling without their ligands, such as NGF and BDNF.

Transphosphorylation is required for the activation of these tyrosine kinase receptors upon interaction with ligands. Insulin and IGF-1 receptors form homodimers at the plasma membrane in the absence of ligands, and ligand binding induces a conformational change in these dimerized receptors, leading to transphosphorylation [13]. However, dimerized F-iIR or F-iIGF1R could not be detected in our pull-down assay (Fig. 5), suggesting that F-iIR and F-iIGF1R failed to form stable dimers. Immunoblot analysis revealed the presence of phosphorylated forms of these receptors in cells transfected with F-iIR and F-iIGF1R, but not iIR and iIGF1R (Fig. 3), indicating that membrane localization is a key step for phosphorylation. Taken together, we speculate that F-iIR (and F-iIGF1R) may transiently interact and form homodimers at the plasma membrane, which induces transphosphorylation and constitutive activation.

F-iIR and F-IGF1R may induce regeneration of dendrite and axon *in vivo*, like F-iTrkB. It is known that there are intrinsic differences in the mechanisms underlying dendritic versus axonal regeneration in adult RGCs [14]. Therefore, a better understanding of the molecular interplay between dendrite and axon regeneration will be crucial to design strategies aimed at achieving complete circuit restoration. We are currently investigating the effects of F-iTrkB on dendritic regeneration, in addition to its effects on promoting axon regeneration. It will also be intriguing to explore potential synergistic effects of F-iIR or F-iIGF1R combined with F-iTrkB on glaucoma symptoms. Our results may have broader implications beyond glaucoma, expanding to other CNS injuries and diseases.

CRediT authorship contribution statement

Akiko Sotozono: Writing – original draft, Methodology, Investigation, Formal analysis, Data curation. **Kazuhiko Namekata:** Writing – review & editing, Writing – original draft, Project administration, Methodology, Investigation, Funding acquisition, Formal analysis, Data curation, Conceptualization. **Xiaoli Guo:** Writing – review & editing, Writing – original draft, Investigation, Funding acquisition, Formal analysis, Data curation. **Youichi Shinozaki:** Writing – review & editing, Investigation, Funding acquisition, Formal analysis. **Chikako Harada:** Writing – review & editing, Funding acquisition, Data curation. **Takahiko Noro:** Writing – review & editing, Funding acquisition, Formal analysis. **Tadashi Nakano:** Writing – review & editing, Project administration, Funding acquisition. **Takayuki Harada:** Writing – review & editing, Writing – original draft, Project administration, Funding acquisition.

Declaration of competing interest

A patent based on the results in this article was filed by the Tokyo Metropolitan Institute of Medical Science (KN and TH are coinventors).

Acknowledgements

This work was supported in part by Japan Society for the Promotion of Science (JSPS) KAKENHI Grants-in-Aid for Scientific Research (JP23K06818 to KN; JP24K12795 to XG; JP22K07368 and JP20KK0366 to YS; JP22K09804 to CH; JP23K09019 to T Noro; JP19KK0229 to T Noro, T Nakano and TH; JP21H04786 and JP24H00583 to TH; JP21H02819 and JP21K18279 to KN and TH); a Shiseido Female Researcher Science Grant (XG), the Takeda Science Foundation (YS and TH) and the Mitsubishi Foundation (TH).

Appendix A. Supplementary data

Supplementary data to this article can be found online at https://doi.org/10.1016/j.bbrep.2024.101799.

References

[1] B.J. Song, L.P. Aiello, L.R. Pasquale, Presence and risk factors for glaucoma in patients with diabetes, Curr. Diabetes Rep. 16 (2016) 124.
[2] R. Ghasemi, A. Haeri, L. Dargahi, Z. Mohamed, A. Ahmadiani, Insulin in the brain: sources, localization and functions, Mol. Neurobiol. 47 (2013) 145–171.
[3] G. Bedse, F. Di Domenico, G. Serviddio, T. Cassano, Aberrant insulin signaling in Alzheimer's disease: current knowledge, Front. Neurosci. 9 (2015) 204.
[4] J. Agostinone, L. Alarcon-Martinez, C. Gamlin, W.Q. Yu, R.O.L. Wong, A. Di Polo, Insulin signalling promotes dendrite and synapse regeneration and restores circuit function after axonal injury, Brain 141 (2018) 1963–1980.
[5] E. Nishijima, S. Honda, Y. Kitamura, K. Namekata, A. Kimura, X. Guo, Y. Azuchi, C. Harada, A. Murakami, A. Matsuda, T. Nakano, L.F. Parada, T. Harada, Vision protection and robust axon regeneration in glaucoma models by membrane-associated Trk receptors, Mol. Ther. 31 (2023) 810–824.
[6] Z.W. Li, S. Liu, R.N. Weinreb, J.D. Lindsey, M. Yu, L. Liu, C. Ye, Q. Cui, W.H. Yung, C.P. Pang, D.S. Lam, C.K. Leung, Tracking dendritic shrinkage of retinal ganglion cells after acute elevation of intraocular pressure, Invest. Ophthalmol. Vis. Sci. 52 (2011) 7205–7212.
[7] L. Della Santina, D.M. Inman, C.B. Lupien, P.J. Horner, R.O. Wong, Differential progression of structural and functional alterations in distinct retinal ganglion cell types in a mouse model of glaucoma, J. Neurosci. 33 (2013) 17444–17457.
[8] L. Feng, Y. Zhao, M. Yoshida, H. Chen, J.F. Yang, T.S. Kim, J. Cang, J.B. Troy, X. Liu, Sustained ocular hypertension induces dendritic degeneration of mouse retinal ganglion cells that depends on cell type and location, Invest. Ophthalmol. Vis. Sci. 54 (2013) 1106–1117.
[9] B. Morquette, P. Morquette, J. Agostinone, E. Feinstein, R.A. McKinney, A. Kolta, A. Di Polo, REDD2-mediated inhibition of mTOR promotes dendrite retraction induced by axonal injury, Cell Death Differ. 22 (2015) 612–625.
[10] M. Pavlidis, T. Stupp, R. Naskar, C. Cengiz, S. Thanos, Retinal ganglion cells resistant to advanced glaucoma: a postmortem study of human retinas with the carbocyanine dye DiI, Invest. Ophthalmol. Vis. Sci. 44 (2003) 5196–5205.
[11] C. Harada, X. Guo, T. Harada, Monogenic gene therapy for glaucoma and optic nerve injury, Neural Regen Res. 20 (2025) 1077-1078.
[12] C.T. Rueden, J. Schindelin, M.C. Hiner, B.E. DeZonia, A.E. Walter, E.T. Arena, K. W. Eliceiri, ImageJ2: ImageJ for the next generation of scientific image data, BMC Bioinf. 18 (2017) 529.
[13] N.O. Yunn, J. Kim, S.H. Ryu, Y. Cho, A stepwise activation model for the insulin receptor, Exp. Mol. Med. 55 (2023) 2147–2161.
[14] J.H. Lim, B.K. Stafford, P.L. Nguyen, B.V. Lien, C. Wang, K. Zukor, Z. He, A. D. Huberman, Neural activity promotes long-distance, target-specific regeneration of adult retinal axons, Nat. Neurosci. 19 (2016) 1073–1084.